EUROPEAN ORGANIZATION FOR NUCLEAR RESEARCH
CERN – ACCELERATORS AND TECHNOLOGY SECTOR

First Measurements of Beam-Induced Heating on the LHC Cryonic System

Brodzinski, K., Tavian L.

Abstract

The Large Hadron Collider (LHC) under operation at CERN is colliding 3.5 TeV hadron beams which are gradually increased in intensity and luminosity. Consequently, beam-induced heating on the beam screens and on the magnet cold masses starts to be observable on the LHC cryogenic system. This paper recalls the cooling principle of the magnet cold masses and beam screens in the LHC standard cells, describes the methods applied for assessing the beam-induced heating, discusses the experimental limitations and compares measurements with expected values.

Geneva, Switzerland
January 2013

First measurements of beam-induced heating on the LHC cryogenic system

Brodzinski K., Tavian L.

Technology Department, CERN, CH-1211 Geneva 23, Switzerland

The Large Hadron Collider (LHC) under operation at CERN is colliding 3.5 TeV hadron beams which are gradually increased in intensity and luminosity. Consequently, beam-induced heating on the beam screens and on the magnet cold masses starts to be observable on the LHC cryogenic system. This paper recalls the cooling principle of the magnet cold masses and beam screens in the LHC standard cells, describes the methods applied for assessing the beam-induced heating, discusses the experimental limitations and compares measurements with expected values.

INTRODUCTION

The Large Hadron Collider [1], installed in a ~27 km-circumference underground tunnel, is composed mainly of superconducting magnets cooled with He II (superfluid helium) at 1.9 K.

With the progressive increase of beam intensity and luminosity, beam-induced heating starts to be clearly visible on the cryogenic system during the LHC operation. The circuits concerned by the beam-induced heating are the 4.6-20 K beam-screen cooling loops on which synchrotron radiation, beam image currents and impingement of photo-electrons are continuously or transitorily deposited, and the 1.9 K cold-mass circuits on which losses of particles are continuously or locally deposited.

The development of LHC operation for physics requires a deep knowledge of the machine characteristics operating with different beam parameters and settings. In particular, the measurement of the beam-induced heating is essential for assessing the beam wall impedance, the quality of the beam vacuum cleaning and scrubbing as well as the margin with particle losses up to resistive transitions of the magnets. Consequently, for both circuit types, heat load measurement methods have been developed and applied.

BEAM-INDUCED HEATING ON BEAM-SCREEN COOLING LOOPS

The beam screens [2] of the LHC are cooled via about 400 parallel cooling loops, i.e. one loop per 53-m half-cell. Figure 1 shows a beam screen cooling loop.
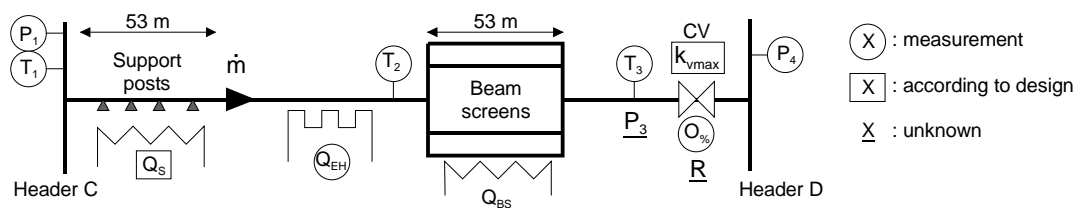

Figure 1 Beam screen cooling loop

A supercritical helium mass-flow $\dot{m}$ at about 0.3 MPa (P_1) and 4.6 K (T_1) enters each loop and is first cooling the heat intercept (Q_S) of the cold-mass support post. An electrical heater Q_{EH} is used to control the temperature at the inlet of the beam screens so as to avoid density wave oscillation in the narrow

beam-screen cooling capillaries. The beam-screen outlet temperature T_3 is adjusted at about 20 K by a control valve. The return flow is collected in a header at 0.13 MPa (P_4).

Measurement method

The beam-induced heating Q_{BS} is estimated by enthalpy balance given by Equation 1, assuming a negligible pressure drop in the cooling loop ($P_3 = P_1$: true if $Q_{BS} < 100$ W). As no flow-meter is available, the mass flow is estimated from the measured valve opening, using the throttled ($P_3/P_4 > 2$) flow characteristics of the equal-percentage control valve. Equation 2 gives the expression for the mass-flow, where k_{vmax} (in m^3/h) is the flow coefficient of the full-open valve; $O_\%$ (in %) is the valve opening and R the valve rangeability. Design values are used for k_{vmax} (0.39 m^3/h) and for Q_S (7.4 W); however for the rangeability, which strongly depends on the clearance between the poppet and the seat of the valve, a lot of dispersion is expected and individual in situ calibrations were performed without beam (Q_{BS}=0).

$$Q_{BS} = \dot{m} \cdot \left(H(T_3, P_1) - H(T_1, P_1) \right) - Q_s - Q_{EH} \tag{1}$$

$$\dot{m} = 1.25 \cdot 10^{-5} \cdot \sqrt{P_1 \cdot \rho(T_3, P_1)} \cdot \frac{k_{vmax}}{R} e^{\left(\frac{O_\%}{100} \cdot ln(R) \right)} \tag{2}$$

Results

Figure 2(a) shows the evolution of the measured beam-induced heating on the beam screens of a LHC sector (~50 loops) during a beam-scrubbing run. These measurements are compared with the expected beam-induced heating due to synchrotron radiation and image currents. Measured values are slightly below the expected ones by about 25 %, except during the first hour following the ramp in beam energy where extra heating up to 25 W appears on some loops due to impingement of accelerated photo-electrons. Figure 2(b) shows the distribution of the valve rangeability assessed via the in situ calibrations. As expected the dispersion is important. In addition, the average rangeability of about 32 is significantly lower than the CERN specified value of 50.
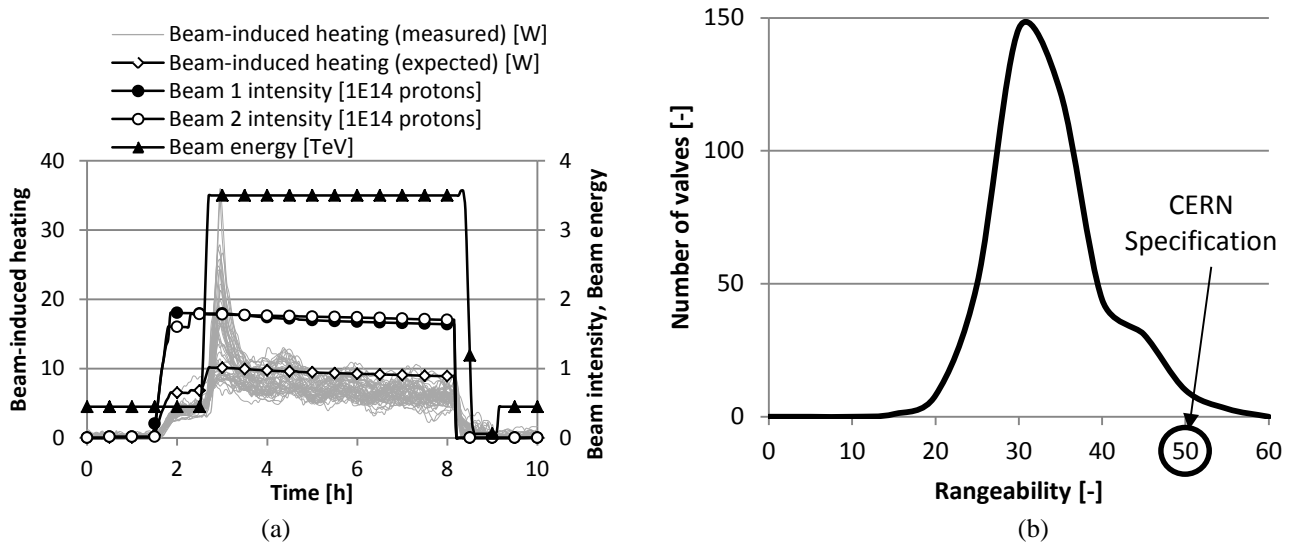

Figure 2 Beam-induced heating evolution in a LHC sector (a) and distribution of valve rangeability (b)
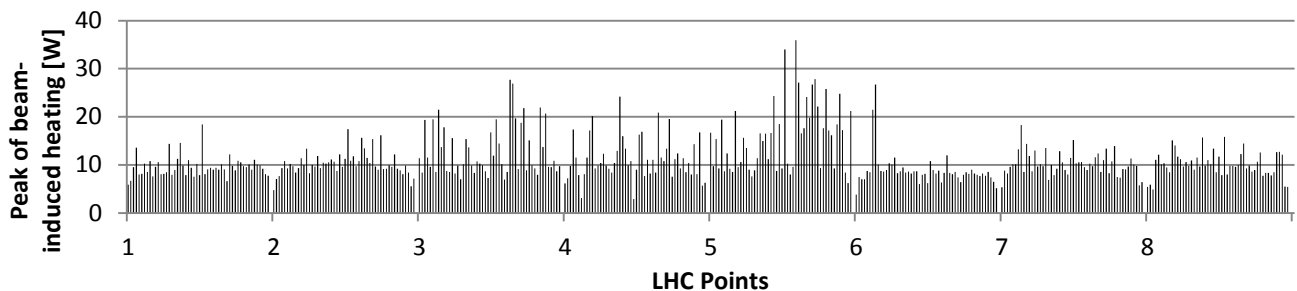

Figure 3 Peak distribution of beam-induced heating around the LHC circumference

Figure 3 shows the peak distribution of the beam-induced heating around the LHC circumference. More photo-electron activity is identified between Point 3 and Point 6 of LHC.

BEAM-INDUCED HEATING ON COLD-MASS CIRCUITS

The cold masses of the main dipoles and quadrupoles of LHC are cooled at 1.9 K in static pressurized superfluid helium (HeII) baths. The cold mass circuit is divided in sub-sectors by hydraulic plugs. The length of a standard sub-sector is 214 m and its superfluid helium inventory is ~800 kg (58 kg per dipole and 25.5 kg per quadrupole). Cold-mass sub-sectors are cooled by two separate and redundant cooling loops, each constituted of a bayonet heat exchanger [3] in which saturated HeII at 1.8 K is flowing and is vaporized by the heat loads. The flow of saturated He II and consequently the temperatures of the pressurized baths are controlled by two Joule-Thomson valves (CV910). Figure 4 shows the cold mass cooling scheme of a standard sub-sector.
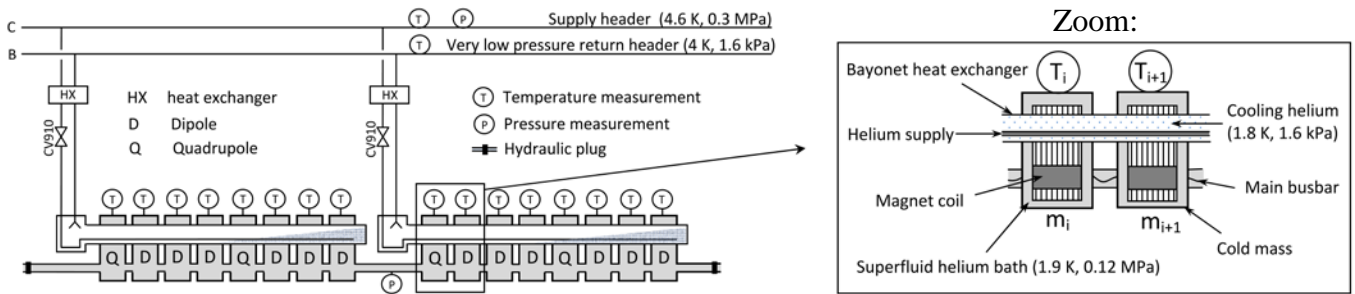

Figure 4 Cold mass cooling scheme of a standard sub-sector

Measurement method
The static pressurized superfluid helium confined in the cold masses follows an isochoric transformation; consequently, the additional heat $Q_{B1.9K}$ entering the cold masses in case of sudden beam loss on the magnet can be measured by the increase in internal energy U of the pressurized HeII– see Equation 3. The input for calculation is taken from temperature sensors T_i installed on each magnet cold-mass and from a pressure sensor P installed on the helium bath. The helium mass m_i of each magnet cold mass is known.

$$Q_{B1.9K} = \sum_{i=1}^{n} m_i \cdot [U_{i2}(T_{i2}, P_2) - U_{i1}(T_{i1}, P_1)] \qquad (3)$$

where: n – number of magnets in concerned sub-sector,
index "1" – values before deposition, index "2" – values after deposition.

Results
Figure 5a shows the evolution of the internal energy in a standard sub-sector after two low-intensity proton beam losses (CV910 in fixed position). For the first beam loss, the sub-sector internal energy increases by 5.5 kJ and corresponds to 84 % of the total beam energy loss. For the second beam loss, the energy increases by 15.9 kJ and corresponds to 93 % of the total beam energy loss. The distribution of energy increase for each magnet in the sub-sector is shown in Figure 5b. The energy deposition is not equally distributed and is more concentrated on the last third of the sub-sector.

A similar type of test was performed with heavy-ion beams on a Dispersion-Suppressor (DS) sub-sector, with partial beam losses on the magnet cold-masses. Figure 6a shows the evolution of energy in the DS sub-sector and the two beam depositions (CV910 in active regulation; due to the fast heat deposition process, the control mode of the valve - fixed position or active regulation – has no influence on the internal energy increase). The first deposition corresponds to 11.3 kJ and the second to 3.3 kJ. Figure 6b shows the distribution of the energy over the DS sub-sector during the first 5 seconds following the first deposition, as well as the beam-loss monitor signals located on the concerned magnet vacuum enclosures. The energy distribution is well in accordance with the beam-loss monitor signals.

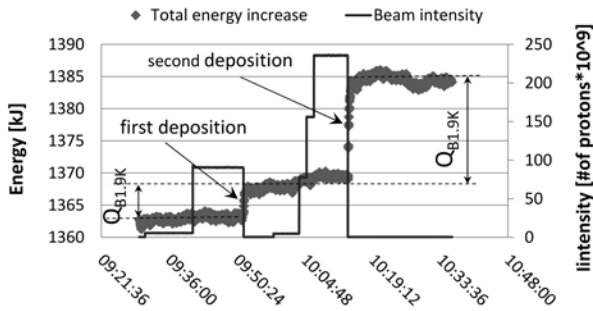None of these tests provoked a magnet resistive transition.

Figure 5a Energy evolution in the standard sub-sector
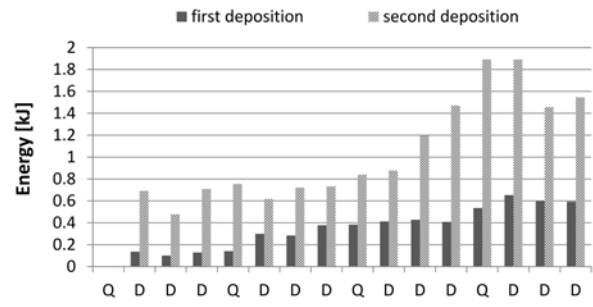

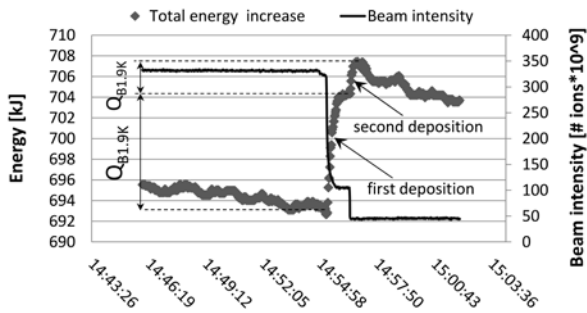Figure 5b Energy increase distribution over the standard sub-sector

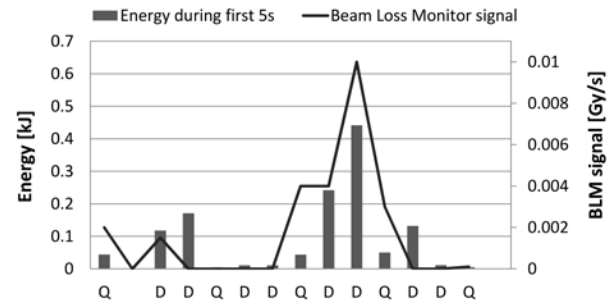Figure 6a Energy evolution in the DS sub-sector

Figure 6b Energy increase distribution over the DS sub-sector during the first 5 s after deposition compared with the beam-loss-monitor signals

CONCLUSIONS

Heat load measurement methods have been developed and applied to assess the beam-induced heating falling on the beam screens and on the magnet cold-masses of the LHC.

In steady-state conditions, the beam-induced heating on the beam screens are presently about 25 % below the expected value. This decrease is mainly due to smaller beam-wall impedance which lowers the image-current heating. Some transient modes create significant additional heating caused by impingement of photo-electrons; this effect will normally decrease with time via beam "scrubbing" of the chamber wall.

Concerning the cold-mass circuits, sudden beam energy depositions of a few kJ are visible by the cryogenic system. The measured profile of energy increase is coherent with beam-loss-monitor signals. Better understanding of energy distribution during the beam losses around the accelerator is needed. The method described opens possibility towards estimation of the quench limits on the magnet coils or superconductor bus-bars.

REFERENCES

1. Brüning O. *et al.* (ed), LHC Design Report, Vol.1, The LHC Main Ring, CERN-2004-003 (2004)
2. Baglin V. *et al,* Cryogenic beam screens for high-energy particle accelerators, presented at this conference
3. Lebrun Ph. *et al,* Cooling strings of superconducting devices below 2 K: the helium II bayonet heat exchanger, Adv. Cryo. Eng. 43A 419-426, (1998)